Energy 206 (2020) 118017

Contents lists available at ScienceDirect

Energy

journal homepage: www.elsevier.com/locate/energy

An integrated two-level demand-side management game applied to smart energy hubs with storage

Seyed Omid Sobhani [a], Siamak Sheykhha [b], Reinhard Madlener [b, c, *]

[a] Department of Energy Engineering, Sharif University of Technology, 11365-11155 Tehran, Iran
[b] Institute for Future Energy Consumer Needs and Behavior (FCN), School of Business and Economics / E.ON Energy Research Center, RWTH Aachen University, 52074 Aachen, Germany
[c] Department of Industrial Economics and Technology Management, Norwegian University of Science and Technology (NTNU), 7491 Trondheim, Norway

ARTICLE INFO

Article history:
Received 18 September 2019
Received in revised form
27 May 2020
Accepted 30 May 2020
Available online 8 June 2020

Keywords:
Smart energy hub (SEH)
Integrated demand-response program
Distributed demand-side management
Storage system

ABSTRACT

Energy hubs, an important component of future energy networks employing distributed demand-side management, can play a key role in enhancing the efficiency and reliability of power grids. In power grids, energy hub operators need to optimally schedule the consumption, conversion, and storage of available resources based on their own utility functions. In sufficiently large networks, scheduling an individual hub can affect the utility of the other energy hubs. In this paper, the interaction between energy hubs is modeled as a *congestion game*. Each energy hub operator (player) participates in a dynamic energy pricing market and tries to maximize his/her own payoff when satisfying energy demand. We propose a distributed algorithm based on a congestion game, which guarantees the existence of a Nash equilibrium. Furthermore, two different types of signaling are developed (price-based, load-based) and simulation results compared. Simulation results show that with the implementation of either setup the peak-to-average ratio between electricity networks and natural gas networks diminishes. An analysis of the results shows that either setup can dominate the other one with regard to generation costs, convergence rate, price level, and stability. Hence, energy providers and consumers can choose a favorable setup based on their respective needs.

1. Introduction

Modern network-based energy systems, such as electricity, natural gas, and district heating, are mostly designed and operated interdependently [1]. Introducing energy hubs as a leading part of future energy networks provides a great opportunity for energy-efficient production, conversion, and storage in such coupled infrastructures, and for system planners, operators, and prosumers to move towards more flexible systems [2]. Numerous studies have been carried out on the concept of the energy hub since Geidl et al. [3] introduced it. Many researchers have studied the combined operation of power, natural gas and heat conversion units. Mancarella provided a general and critical overview of the latest models and assessment techniques available today for the analysis of multi-energy systems, and in particular distributed multi-generation systems (DMGS) [4].

Propagation of the market penetration level of combined heat and power (CHP) and micro-CHP in multiple countries, along with the utilization of smart grids (SGs) in the electricity networks, has paved the way for a smart natural gas infrastructure. As a result, the developing of modern and new methods for Demand-Side Management (DSM) in electricity and natural gas networks is crucial. Game theory has been used to solve many problems in DSM. Sheikhi et al. [5] used game theory to model DSM among smart energy hubs (SEHs). Simulation results showed a reduction in both the peak-to-average ratio (PAR) of the total electricity demand in the Nash equilibrium and the hub users' energy bills. Sheikhi et al. [6] proposed a cloud-computing energy management framework based on integrated demand-side management (IDSM). This IDSM model is based on game theory, which enables an efficient data processing and information management. Bahrami and Aminifar [7] studied the potential of energy hubs for power system regulation services. They proposed an auction to participate in regulation services and modeled the interaction among energy hubs as a non-

* Corresponding author. Institute for Future Energy Consumer Needs and Behavior (FCN), School of Business and Economics / E.ON Energy Research Center, RWTH Aachen University, Aachen, Germany.
E-mail address: RMadlener@eonerc.rwth-aachen.de (R. Madlener).

https://doi.org/10.1016/j.energy.2020.118017
0360-5442/

Nomenclature

$a_i^{e/h}$	Charge/discharge rate of electric/heat storage devices of i^{th} energy hub
$b_i^{e/h}$	Initial energy level of electric/heat storage devices of i^{th} energy hub
$CAP_i^{e/h}$	Capacity of electric/heat storage devices of i^{th} energy hub
$C^{e/g}$	Generation cost of electricity/gas
$CF_{\alpha\beta}$	Coupling/conversion factor between input energy carrier α and output energy carrier β
$[\mathbf{d}]$	Dispatch factor matrix of different input power
$D_i^{e/h}$	Energy level of electric/heat storage devices of i^{th} energy hub
$[\dot{\mathbf{E}}]$	Storage flow
$\mathscr{F}_i$	Feasible set of strategy vectors for i^{th} user
$\mathbf{I}^{e/h}$	Electricity/heat demand vectors
$m.u.$	Monetary unit
$\mathscr{N}$	Set of users (hubs)
$p.u.$	Per unit
$pr^{e/g}$	Price of electricity/gas per unit
$P_{\alpha,i}$	Input/output power of i^{th} energy hub
$\mathbf{S}$	Strategy vector
$[\mathbf{ST}]$	Storage coupling matrix
t	Time slot
T	Set of time slots
U	Utility function
$[\boldsymbol{\eta}]$	Efficiency coefficient matrix of equipment
α, β, ω	Different types of energy carriers (input α, output β)
κ_i	Proportion of i^{th} user's energy consumption

cooperative game with coupling constraints.

For some time, scholars have been developing market frameworks for efficiently managing demands and exploiting consumer flexibility in DS programs. Mohsenian Rad et al. [8] used game theory to formulate an energy consumption scheduling game and showed that optimal scheduling of a single utility company with multiple consumers occurs in the Nash equilibrium. Lu et al. [9] designed a transaction mechanism among retailers and consumers in a regional energy market. They demonstrated the existence and uniqueness of the Nash equilibrium by means of a distributed algorithm with an overarching particle swarm optimization algorithm. Liang et al. [10] proposed a monotonically distributed model and an optimization algorithm for the autonomous energy management of multi-residential energy hubs. Li et al. [11] used a mathematical program with an equilibrium constraint (MPEC) model to identify the strategic behavior of players in an energy hub (EH) in the electricity market and the heating market on two levels. Huang et al. [12] used a game-theoretical approach for optimal scheduling. They tested it for two case studies; in the first group, they showed that the system cost changes with the total electric load. Results for the second group reveal that the optimal scheduling result of the system is influenced by the variation of the seasons.

In decentralized models, the instantaneous price changes are shared among all the demands and, as a consequence, energy allocation based on their self-determining decision-making approaches is triggered by demand signals [13]. "Integrated demand response" helps multi-energy systems, such as natural gas, district heat/cooling, biomass, and electric power systems, to back up each other in order to constitute a more economical entity. Furthermore, users can exploit their response capability without any loss of energy users' comfort [14]. Most of the studies focus on optimal operation of energy hubs by considering demand response (DR). Mukherjee et al. [15] analyzed a power-to-gas EH in two steps: optimal sizing of the components of the EH and the development of a complex optimization model to optimize the operation of the hub. Zhang et al. [16] scrutinized the optimal network capacity and the distribution of the CHP-based distributed generation based on urban energy distribution networks by means of an integrated system dispatch model. Tingji et al. [17] proposed a single EH for managing battery storage and a solar PV system with two control strategies for grid-mode and island-mode. Aghamohamadi and Mahmoudi [18] developed an adaptive robust integrated bidding strategy to model EHs. Consequently, the EHs can bid in multiple energy markets simultaneously in order to optimize their benefits/costs. Bahrami et al. [19] studied the existence and uniqueness of the Nash equilibrium and designed an online distributed algorithm to achieve that equilibrium. They showed that the proposed algorithm can increase the EHs' average payoff and the technical performance of the energy network by reducing the PAR for both electricity and natural gas. Noor et al. [20] proposed a game-theoretical approach for a DSM model, incorporating storage components and taking into account the supply constraints in the form of power outages. The proposed model is able to both reduce the PAR and smooth the dips in load profiles caused by supply constraints.

The temporal and spatial distribution of the DR capacity can influence the bidding behavior of demand response aggregators (DRAs) in the electricity market. Pipattanasomporn et al. [21] investigated how demand response opportunities of selected household appliances in the U.S. over different time intervals can be controlled. Motalleb and Ghorbani [22] developed a game-theoretical framework where DRAs took part in a competition to sell their energy which they had previously stored in residential storage devices. They report on a case study for the island of Muai (Hawaii, United States) where they calculate local power demand levels using hot water consumption data (15 min resolution), total loads using public statistical data, and applying a Bayesian approach to derive probability distributions for DRAs. Furthermore, residential electricity consumption is affected not only by DR signals but also by energy end-users' behavior. This behavior encompasses lack of knowledge, forecasting of weather circumstances etc. [23]. Zhen et al. [24] proposed a classification pattern and PSO optimization weights to forecast solar power using sky images. Li et al. [25] introduced a PV decoupling method to estimate volatile actual load and intermittent output of solar PV.

This paper focuses on extending the works in [5] and [6] by exploiting storage technologies. One major concern regarding the simulation of a system of interconnected SEHs which are equipped with storage devices is that of oscillation, which prevents the system from converging properly. The main challenge that we address in this paper is to propose a novel distribution algorithm which converges properly. The main contribution of this paper to the literature can be summarized as follows:

- A distributed integrated DSM program is proposed in a dynamic pricing market set-up for electricity and natural gas networks. In the proposed algorithm, each of the SEHs independently bids for its daily profile to the network operator, and other information related to the internal operation of SEHs is kept private.
- Equipping SEHs with storage devices can impose oscillation in the system and prevent the common algorithm from converging

properly. We propose a novel modification function in our algorithm which helps the algorithm to converge.
- To coordinate the operation of individual SEHs, two different types of signaling are developed and simulation results are compared. This is significant for those energy suppliers which provide both electricity and natural gas.
- The proposed method is considerably robust against any probable structural change to the problem. It means that each hub can choose and update its parameters independently and it can apply any strategy without communicating with any of the other hubs.

The remainder of this paper proceeds as follows. In section 2, the system model (comprising the heat and electricity demand, energy storage module, and SEH concept) is presented. Section 3 gives an overview of the decentralized design of the SEH and describes the algorithm used in this paper for arranging and modeling the SEH. Furthermore, a load-based setup and a price-based setup are identified in this section. Simulation results are presented in section 4. Section 5 concludes.

2. System model

In this section we introduce the main parts of the model. First, we introduce the concept of demand vectors. Second, the storage model in the smart energy hub is described. Finally, we describe the energy hub model which is equipped with conversion and storage devices.

2.1. Heat and electricity demand

Consider $\mathscr{T}$ to be the set of time slots and $\mathscr{N}$ to be the set of energy end-users (consumers, agents), where $T := |\mathscr{T}|$ and $N := |\mathscr{N}|$. We assume that each user has some controllable/shiftable electric loads as well as must-run loads. For each user $i \in \mathscr{N}$ the electric energy and heat consumption vectors are defined as follows:

$$\mathbf{l}_i^e = \left[l_i^{e,1}, \ldots, l_i^{e,t}, \ldots, l_i^{e,T} \right], \tag{1}$$

$$\mathbf{l}_i^h = \left[l_i^{h,1}, \ldots, l_i^{h,t}, \ldots, l_i^{h,T} \right], \tag{2}$$

where $l_i^{e,t}$ and $l_i^{h,t}$ are amounts of electricity and heat, respectively, needed by the i^{th} consumer at time t. Note that we assume predetermined daily electricity and heat demand vectors $\mathbf{l}_i^e$ and $\mathbf{l}_i^h$, for each consumer's appliances. Furthermore, a standard load profile has been used which is described in section 3.3. below.

2.2. Energy storage model

Let a_i^t be the energy charging or discharging rate of the i^{th} consumer's battery at time slot t. For this reason, the energy storage vector for the i^{th} consumer's battery, considering the maximum possible charging and discharging rate in each time slot, is:

$$\mathbf{a}_i^e = \left[a_i^{e,1}, \ldots, a_i^{e,t}, \ldots, a_i^{e,T} \right] \tag{3}$$

$$-a_{i,max}^e \le a_i^{e,t} \le a_{i,max}^e, \tag{4}$$

where $a_{i,max}^e$ is the maximum electricity charge or discharge rate for one time slot. $a_i^{e,t} > 0$ means that the i^{th} consumer is trying to charge his/her battery and $a_i^{e,t} < 0$ means he/she is trying to discharge it.

The charging and discharging schedule for each battery depends on the schedule in the previous time slots. To prevent overcharging, the battery's stored energy after charging cannot be more than CAP_i^e, the maximum battery capacity of user i. In order to prevent discharging the battery too much, the residual stored energy of the battery after discharging must be greater than a specific threshold, which is supposed to be zero. Therefore, the constraint is:

$$0 \le b_i^{e,0} + \sum_{j=1}^{t} a_i^{e,j} \le CAP_i^e, \quad \forall t \in \mathscr{T}, \tag{5}$$

where b_i^0 stands for the battery's initial charge level. Moreover, we suppose that the most desirable charge level, b_i^T, is known in advance by each consumer. As each consumer has information about the desirable charge level and the initial charge level, the amount of energy required for charging a consumer's battery, D_i^e, can be obtained as follows:

$$D_i^e = b_i^{e,T} - b_i^{e,0}. \tag{6}$$

Accordingly, for charging and discharging the battery, we have the constraint:

$$\sum_{t=1}^{T} a_i^{e,t} = D_i^e. \tag{7}$$

We can define a similar scheduling vector for the heat storage devices as follows:

$$\mathbf{a}_i^h = \left[a_i^{h,1}, \ldots, a_i^{h,t}, \ldots, a_i^{h,T} \right] \tag{8}$$

with the following constraints:

$$-a_{i,max}^h \le a_i^{h,t} \le a_{i,max}^h \tag{9}$$

$$0 \le b_i^{h,0} + \sum_{j=1}^{t} a_i^{h,j} \le CAP_i^h, \quad \forall t \in \mathscr{T} \tag{10}$$

$$D_i^h = b_i^{h,T} - b_i^{h,0} \tag{11}$$

$$\sum_{t=1}^{T} a_i^{h,t} = D_i^h. \tag{12}$$

2.3. Smart energy hub model

A smart energy hub is an energy hub which is located in a smart grid that is equipped with smart meters for natural gas and electricity networks and that employs suitable communication infrastructures (Fig. 1). All data needed are interchanged among the smart meter infrastructure, using suitable communication protocols such as KNX, ZigBee, or Z-Wave [26]. Power conversion through the hub can be determined from the following equation:

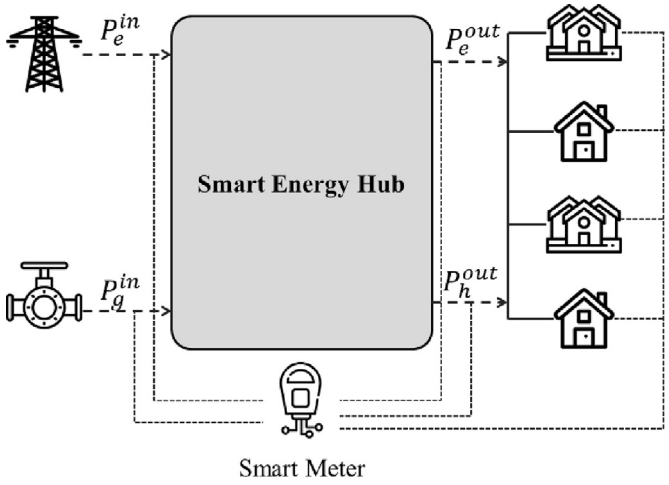

Fig. 1. Architecture of a simple smart energy hub.

$$\begin{bmatrix} P^{out}_{\alpha,i} \\ P^{out}_{\beta,i} \\ \vdots \\ P^{out}_{\omega,i} \end{bmatrix} = \begin{bmatrix} CF_{\alpha\alpha} & CF_{\beta\alpha} & \dots & CF_{\omega\alpha} \\ CF_{\alpha\beta} & CF_{\beta\beta} & \dots & CF_{\omega\beta} \\ \vdots & \vdots & \ddots & \vdots \\ CF_{\alpha\omega} & CF_{\beta\omega} & \dots & CF_{\omega\omega} \end{bmatrix} \begin{bmatrix} P^{in}_{\alpha,i} \\ P^{in}_{\beta,i} \\ \vdots \\ P^{in}_{\omega,i} \end{bmatrix} \tag{13}$$

where $P^{in}_{\alpha,i}$, $P^{in}_{\beta,i}$ … $P^{in}_{\omega,i}$ are the input energy carriers' power corresponding to the ith SEH. $P^{out}_{\alpha,i}$, $P^{out}_{\beta,i}$, …, $P^{out}_{\omega,i}$ are the output energy carriers' power and $CF_{\alpha\beta}$ represents the coupling factor between input energy carrier α and the output energy carrier β's energy flow. Equation (13) can be written as:

$$[\mathbf{P}_i^{out}] = [\mathbf{CF}] \times \left[\mathbf{P}_i^{in}\right]. \tag{14}$$

Energy hubs may be equipped with energy storage devices on the input side or the output side of converters. In this case, we can mathematically model the SEH as follows:

$$[\mathbf{P}_i^{out}] = [\mathbf{CF}{-}\mathbf{ST}] \begin{bmatrix} \mathbf{P}_i^{in} \\ \dot{\mathbf{E}} \end{bmatrix}, \tag{15}$$

where **ST** is the coupling storage matrix which indicates the power flow in storage devices. $\dot{E} = E_t - E_{t-1}$ is the vector of the charging/discharging rate in the storage devices. By assuming the efficiency of a converter to be constant, coupling factors can be calculated by multiplying the dispatch factors and the efficiency of the equipment, $[\mathbf{CF}] = [\eta] \times [\mathbf{d}]$. Each element in [**CF**] takes a value less than 1.

For the sample SEH presented in Fig. 2, the total electric energy demand, $P^{in}_{e,i}$, and total demand for natural gas, $P^{in}_{CHP,i} + P^{in}_{b,i}$, which user i purchases in each time slot t from the energy provider/s (to supply that user's appliances and storage devices) can then be constrained as follows:

$$l^e = P_e^{out} = \eta_{Tr} P_e^{in} - \frac{a^e}{\eta_e} + \eta^e_{CHP} P^{in}_{CHP} \tag{16}$$

$$l^h = P_h^{out} \le \eta^h_{CHP} P^{in}_{CHP} + \eta_b P^{in}_b - \frac{a^h}{\eta_h}, \tag{17}$$

where η_{Tr}, η_b, η^e_{CHP}, and η^h_{CHP} denote the efficiency of transformer, boiler, electric efficiency of CHP, and heat efficiency of CHP, respectively. We model the charging/discharging losses of the battery and the heat tank as η_e and η_h, respectively, as follows:

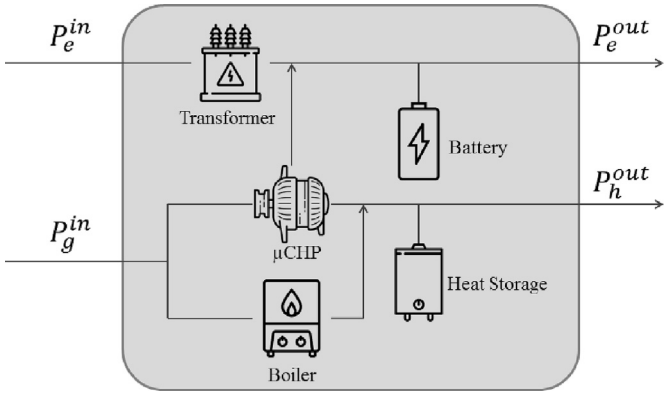

Fig. 2. Exemplary smart energy hub equipped with battery and heat storage.

$$\eta_{e/h} = \begin{cases} \eta^{+}_{e/h}, & 0 \le a_{e/h} \\ \dfrac{1}{\eta^{-}_{b/h}}, & a_{e/h} < 0 \end{cases}. \tag{18}$$

Finally, we constrain the operational capacity of the transformer, the CHP unit, and the boiler with the following equations:

$$0 \le P^{in,t}_{Tr,i} \le P^{max}_{Tr,i} \tag{19}$$

$$0 \le P^{in,t}_{CHP,i} \le P^{max}_{CHP,i} \tag{20}$$

$$0 \le P^{in,t}_{b,i} \le P^{max}_{b,i}. \tag{21}$$

Finally, the feasible energy consumption and storage schedule of the i^{th} consumer can be defined as follows:

$$\mathscr{T}_i = \left\{ \mathbf{P}_i^{in,e}, \mathbf{P}_i^{in,g}, \mathbf{a}_i^e, \mathbf{a}_i^h \,\middle|\, 4 \text{ to } 7 \;-\; 9 \text{ to } 12 \;-\; 16 \text{ to } 21 \right\}. \tag{22}$$

3. Distributed configuration

In this section, using a generation cost model, we introduce two different decentralized configurations in which consumers independently maximize their utility by optimizing the energy storage and consumption strategy vectors based on their individual objective functions. In both setups, the load-based (section 3.2) and the price-based (section 3.3) one, each energy hub operator participates in a dynamic energy pricing market with a different signaling type for the optimization (price-based, load-based; see below). A coordinating agent coordinates the bids of all users. As is shown in Fig. 3, smart energy hubs obtain their demand for electricity and gas from the electricity and gas grids. All SEHs are connected to a data center to which they transfer information based on the model's configuration. Note that in this figure, solid and dashed lines represent the energy and information flows, respectively.

3.1. Generation cost and pricing model

Assume that generating P^e_t units of electric power costs $C^e(P^e_t)$, a

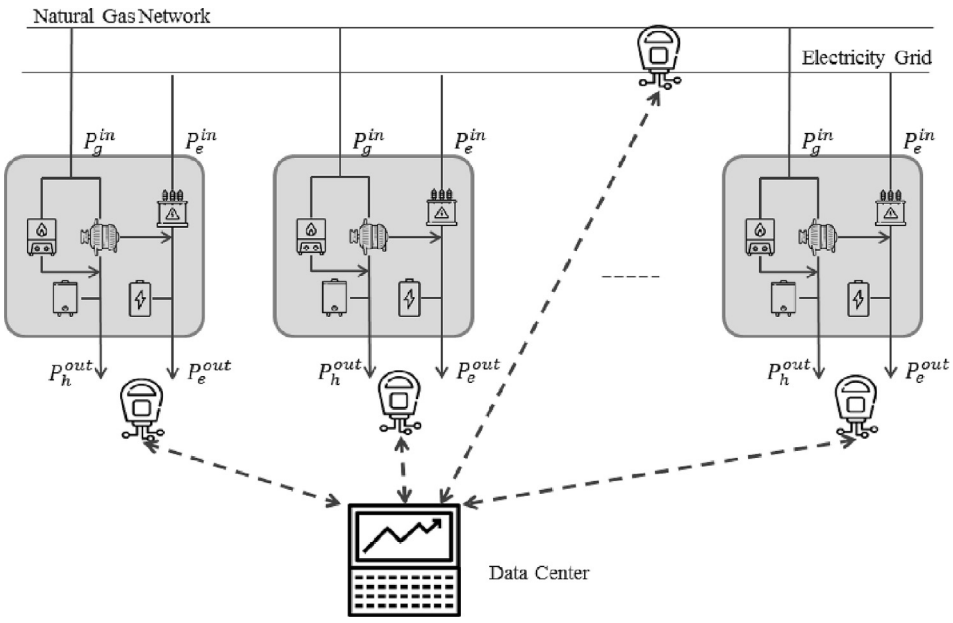

Fig. 3. Illustration of scheduling in integrated demand-side management.

specification which is commonly discussed in the literature [27,28] is:

$$C^e\left(P_t^e\right) = \delta^e\left(P_t^e\right)^2 + \varepsilon^e P_t^e, \tag{23}$$

where δ^e and ε^e are well-known positive coefficients often used in the smart grid and the energy hub literature. Likewise, we can calculate the total cost of electricity for each time interval as follows:

$$C^e_{total,t} = C^e\left(\sum_{i=1} P^e_{i,t}\right). \tag{24}$$

For each time step, the i^{th} consumer would be charged according to the ratio of his/her electricity consumption to the total demand. Let $\kappa^e_{i,t}$ represent the i^{th} consumer's electricity consumption to the network's load ratio at time slot t:

$$\kappa^e_{i,t} = \frac{P^e_{i,t}}{\sum_{j=1}^{N} P^e_{j,t}}. \tag{25}$$

In the load-based setup (see section 3.2 below), we suppose that the i^{th} consumer would be charged proportionally to the total electricity demand costs of the system, i.e.

$$C^e_{i,t} = \kappa^e_{i,t} C^e_{total,t}. \tag{26}$$

In Eq. (26), it is obvious that the payment of the i^{th} consumer depends on the total electricity cost of the system and that consumer's proportion of the electricity demand. For example, if the i^{th} consumer uses twice as much electrical energy as the j^{th} consumer in each time slot t, then consumer i must pay twice as much for the electricity as consumer j. Analogously, with the same ratiocination, we can derive a natural gas sharing model as follows:

$$C^g\left(P_t^g\right) = \delta^g\left(P_t^g\right)^2 + \varepsilon^g P_t^g. \tag{27}$$

$$C^g_{total} = C^g\left(\sum_{i=1} P^g_{i,t}\right). \tag{28}$$

$$\kappa^g_{i,t} = \frac{P^g_{i,t}}{\sum_{j=1}^{N} P^g_{j,t}}. \tag{29}$$

$$C^g_{i,t} = \kappa^g_{i,t} C^g_{total,t}. \tag{30}$$

In the price-based configuration (see section 3.3 below), the utility function depends on the price of the energy carriers. The price of each unit of generated energy is simply calculated as follows:

$$Pr^e_{t,p.u} = \frac{C^e_t\left(P^e_t\right)}{P^e_t}, \tag{31}$$

$$Pr^g_{t,p.u} = \frac{C^g_t\left(P^g_t\right)}{P^g_t}. \tag{32}$$

where $Pr^e_{t,p.u}$ and $Pr^g_{t,p.u}$ are the prices per unit of generated electrical energy and natural gas, respectively.

3.2. Setup I: load-based setup

In this setup, the coordinating agent, receives the electricity and natural gas demand of all users, and the aggregated load profiles of the networks are shared between users in each iteration. Therefore, users update their strategy vectors, based on this information and their modified objective function, which allows to maximize their utility (minimize their payment).

For each user $i \in \mathcal{N}$, utility gains arise from negative energy payments (i.e. cost savings) over T time slots. As total demand affects the energy price, the energy payment that each user pays to the energy provider depends on both their own energy demand and also on the other users' energy demands. Eq. (33) represents the strategy vector of user $i \in \mathcal{N}$:

$$\mathbf{S}_i = \left[\mathbf{P}_i^e, \mathbf{P}_i^g, \mathbf{a}_i^e, \mathbf{a}_i^h\right]. \tag{33}$$

Following this, by plugging Eq. (26) and Eq. (30) into Eq. (33), the final utility function for user i can be derived as follows:

$$U_i(\mathbf{S}_i, \mathbf{S}_{-i}) = -C_i = \\ -\sum_{t=1}^{T}\left[\kappa_{i,t}^e\left(\delta^e\left(P_{i,t}^e + P_{-i,t}^e\right)^2 + \varepsilon^e\left(P_{i,t}^e + P_{-i,t}^e\right)\right)\right. \\ \left.+\kappa_{i,t}^g\left(\delta^g\left(P_{i,t}^g + P_{-i,t}^g\right)^2 + \varepsilon^g\left(P_{i,t}^g + P_{-i,t}^g\right)\right)\right], \tag{34}$$

where $P_{-i,t}^e$ and $P_{-i,t}^g$ denote the sum of electricity and natural gas demand of all users except user i at time slot t, respectively. In short, $P_{-i} = \sum_j P_j \big| j \neq i$. $\mathbf{S}_i$ consists of the load profile vectors of energy consumption of user i. $\mathbf{S}_{-i} := [\mathbf{S}_1, \mathbf{S}_2, \ldots \mathbf{S}_{i-1}, \mathbf{S}_{i+1} \ldots, \mathbf{S}_N]$ denotes the vectors of the electricity and natural gas load profiles that all users except user i choose. Note that in the utility function (Eq. (34)), the cost of battery lifetime reduction is neglected.

3.3. Setup II: price-based setup

In this setup, the coordinating agent receives the electricity and natural gas demand of all users and calculates the price of each carrier for each time slot based on Eqs. (31) and (32). Users will be informed about the price profiles of different energy carriers in each iteration and will update their strategies. Consequently, they can maximize their utility according to the price profile of different energy carriers.

The utility function of each user $i \in \mathcal{N}$ over all time slots considered can be identified as a negative payment. The energy bill of each user simply depends on the energy price per unit – which is calculated by the independent coordinating agent – and the user's own energy demand. Using Eqs. (31) and (32), we can rewrite Eq. (34) for this configuration as follows:

$$U_i(\mathbf{S}_i, \mathbf{S}_{-i}) = -C_i = -\sum_{t=1}^{T}\left[Pr_{t,p.u}^e \times P_{i,t}^e + Pr_{t,p.u}^g \times P_{i,t}^g\right]. \tag{35}$$

3.4. Game-theoretical model

In this paper, we describe a congestion game for the energy hubs' interaction game. A game is said to be a congestion game if each player's payoff depends on the resource he/she chooses and the number of players choosing the same resource [30]. In a distributed SEH system, each consumer $i \in \mathcal{N}$, independently of the others, tries to minimize his/her energy costs, which leads to a non-cooperative energy consumption and storage (NCECS) game among end-users. This game is defined by three components:

$$G = \{\mathcal{N}, \{\mathcal{F}_i\}_{i\in\mathcal{N}}, \{U_i\}_{i\in\mathcal{N}}\} \tag{36}$$

- The players, who are the consumers in the set $\mathcal{N}$;
- The strategy of each consumer $i \in \mathcal{N}$, which corresponds to the energy consumption and storage vectors, $\mathbf{S}_i \in \mathcal{F}_i$; and
- The utility function U_i of each consumer $i \in \mathcal{N}$ as specified in Eq. (34) or (35).

Based on the definition of the utility and strategies in the NCECS game, in order to maximize the utility function, each consumer tries to select his/her energy consumption, conversion, and battery charging/discharging schedules. The best response strategy is when the i^{th} player (consumer) aims at maximizing his/her utility function, while assuming that all other consumers' strategies are fixed. For each consumer $i \in \mathcal{N}$, the best response strategy is:

$$S_i^{best} \in \text{argmax}_{\mathbf{S}_i \in \mathcal{F}_i} U_i. \tag{37}$$

Thus, for any consumer, any best response strategy, $\mathbf{S}_i^*$, is as least as good as every other strategy in $\mathcal{F}_i$ when the strategies of the other users, $\mathbf{S}_{-i}$, are fixed. For the defined NCECS game, the Nash equilibrium is then defined as follows.

Definition. Consider the NCECS game, with utility function U_i given by Eq. (34) or (35). A vector of strategies $\mathbf{S}^*$, if and only if it satisfies the following set of inequalities, constitutes a Nash equilibrium of the NCECS game.

$$U_i(\mathbf{S}_i^*, \mathbf{S}_{-i}^*) \geq U_i(\mathbf{S}_i, \mathbf{S}_{-i}^*) \quad \forall(\mathbf{S}_i) \in \mathcal{F}_i, \forall i \in \mathcal{N}. \tag{38}$$

A Nash equilibrium of the NCECS game represents a status in which no user can increase his/her utility by changing the energy consumption and storage schedules while the strategy of all other consumers are fixed. Now, we can propose the NCECS game algorithm as shown in Table 1. This is an iterative-based solution which is applied by the coordinating agent. In the first step, some coefficient and variables are initialized. In each iteration, the coordinating agent announces the modified aggregated load/price profile of the energy carriers to each agent (hub). Each agent optimizes his strategy vector based on the announced load/price profiles and announces his/her demand profile and the value of the objective function. Again, the coordinating agent calculates the modified aggregated load/price profiles and announces it to the agents. This procedure is repeated until the value of the objective function of all agents in two consecutive iterations differs less than the defined value (Δ).

4. Performance evaluation

Five hubs are considered in this model application, which are connected to electricity and natural gas networks (Fig. 3), and one electricity company and one natural gas company each exist in the proposed energy system. $T = 24$ time slots have been considered. The electrical and heat load demands for a sample energy hub are considered for a sunny summer day in Germany (Fig. 4) and each considered hub follows this pattern with a coefficient as presented in Table 2. For all hubs, the efficiency coefficient of the equipment are parameterized in Table 3. Furthermore, for the sake of simplicity, heat demand is assumed to be satisfied instantly in the hubs.

The optimization problem for each hub includes 24 equality and 456 inequality constraints, respectively. They have 168 decision variables. All simulations were performed in MATLAB-R2015b, running in Windows 10 64-bit, using a personal computer equipped with an Intel Core i7 processor. The proposed algorithm is run for different numbers of SEHs. Fig. 5 illustrates that the running time increases slightly with the number of SEHs. Hence, it can be concluded that the proposed method may also be used for a system with a large number of SEHs.

4.1. General system operation

Fig. 6 shows the total electrical power input in the presence and

Table 1
Algorithm of the proposed method.

1.Initialization: $j = 1$, $\Delta = 10^{-2}$, cost coefficients and $S_i = 0$
2. Repeat algorithm
3. Receive modified aggregated P^e_{in} and P^g_{in} or the price profile of the carriers
4. Compute for each hub (in parallel)
5. Update strategy vector S^k_i according to P^e_{in} and P^g_{in} using S^0_i
6. Update power inputs according to S_i
7. End
8. $S^0_i = S^k_i$
9. $j = j + 1$
Repeated until for all users $\left|U^{j+1}_i - U^j_i\right| \le \Delta$

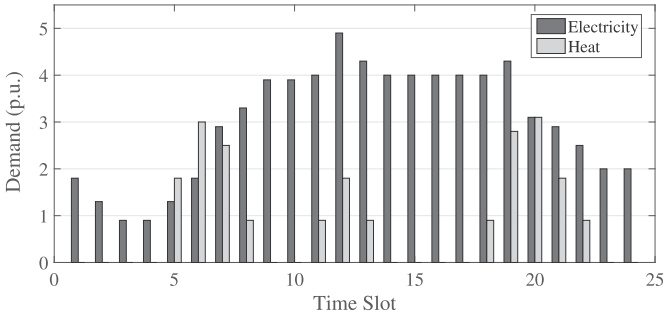

Fig. 4. Electricity and heat demand for a sample energy hub (per unit).

Table 2
Demand coefficients and storage capacity of the five different energy hubs considered.

	Hub 1	Hub 2	Hub 3	Hub 4	Hub 5
L_e coefficient	1	0.8	1.2	0.8	1.2
L_h coefficient	1	0.8	1.2	0.8	1.2
Heat storage capacity (p.u)	4	55	3	3.5	4.5
Battery capacity (p.u)	5	6	55	4.5	4

Table 3
Simulation constants.

$\eta_{t,i}$	$\eta_{e,chp}$	$\eta_{h,chp}$	η_{boiler}
0.99	0.3	0.4	0.75

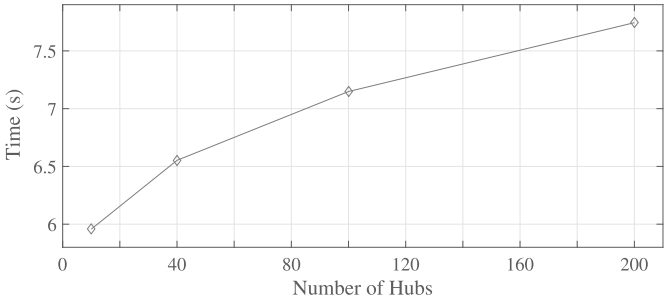

Fig. 5. Average time required to reach proper convergence.

absence of two configurations of the SEHs. In both the load-based and the price-based scheme, aggregated electric power input into the hubs, which is equal to the electrical power generated by the suppliers, is not only reduced during peak hours but is also increased in off-peak hours. It means that the consumers buy electricity during the off-peak periods, store it in their battery, and use it during the peak periods of a day. Fig. 7 shows the total natural gas power input into the hubs, which is equal to the natural gas that the utility company sells in the aforementioned scheme. Aggregate gas power input is flattened by using the SEH. Thus, end-users prefer to buy more natural gas during electricity network peaks and to convert it into electricity, as this is cheaper than buying electricity from the grid.

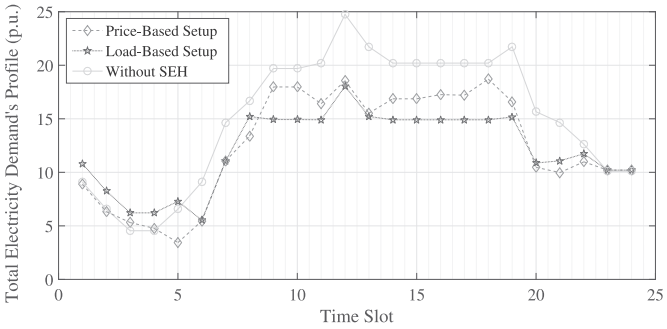

Fig. 6. Sum of electrical power input (per unit) for the two setups and without SEH.

Fig. 6 indicates that the peak demand profile of electricity for load-based and price-based setups is reduced by 27.1% and 24.4%, respectively. As Fig. 7 shows, the peak of the demand profile of the natural gas network for both load-based and price-based setups is increased by 24.8%.

The PAR index is used to quantify imbalances in the daily energy consumption's load base. As is shown in Eq. (39), the PAR is the ratio of the average energy consumption in peak time to the energy consumption during one day:

$$PAR = \frac{max P^{in}_{\alpha}(t)}{\sum_{t=1,2,\ldots 24} P^{in}_{\alpha}(t) \Big/ 24}. \tag{39}$$

The PAR for electricity without the SEH is 1.64. With the SEH, it is

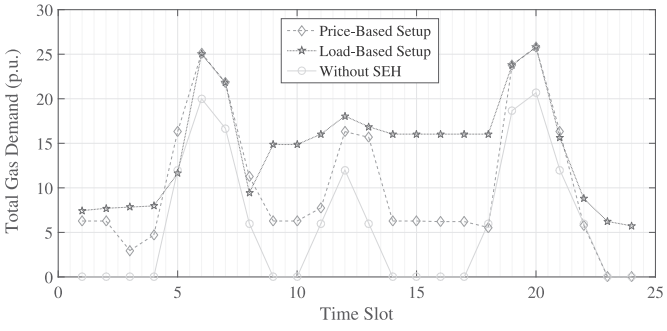

Fig. 7. Sum of natural gas power input (per unit) for the two setups and without SEH.

1.48 for the load-based setup and 1.49 the price-based setup, respectively, which reflects a 9.3% decrease in the aggregate load demand for electricity in the load-based setup and a 8.5% decrease in the price-based setup.

The PAR for natural gas without SEH is 3.49; with the SEH it amounts to 1.79 for the load-based setup and 2.48 for the price-based setup, respectively, which reflects a 48.7% decrease in the aggregate load demand for natural gas in the load-based setup and a 28.9% decrease in the price-based setup. It implies that applying both configurations of the SEH will be appropriate for the natural gas network.

As is shown in Figs. 6 and 7, the price-based setup results in more fluctuation in the aggregated load profile than the load-based setup does, which can induce more instability in energy networks. Fig. 8 demonstrates the energy price profiles for different configurations. As is shown in this figure, on the one hand, the prices in the electricity network decrease during peak times of the day due to the reduction in electricity consumption. On the other hand, gas prices during the day increase due to the increase in gas consumption. However, simulation results show a reduction in the energy bills in both configurations. As an illustration, at the end of the simulated day, User 1 has to pay 3.6×10^3 units of money ($m.u.$) to the energy providers without the implementation of SEHs, whereas these payments reduce to $2.92 \times 10^3 m.u.$ and $2.80 \times 10^3 m.u.$ for the load-based setup and the price-based setup, respectively.

Fig. 9 represents the total energy generation cost for conventional systems (without SEH) and the two proposed setups at different times of the day. As is shown in this figure, the generation cost for the conventional system is much higher than for the other setups at most of the time during the day. For instance, the generation cost without implementing the SEH at 12:00 and 13:00 h is at least 28.2% and 25.1%higher than the other setups. The total generation cost for the day without implementing the SEH is $1.68 \times 10^4 m.u.$, for the load-based setup it is $1.48 \times 10^4 m.u.$ and for the price-based setup $1.42 \times 10^4 m.u.$, which implies a reduction of 11.9% and 15.5%, respectively.

4.2. The load-based setup

Fig. 10 presents the convergence process of total electricity and natural gas demand for 5 different sample time slots by implementing the load-based setup. Fig. 11 shows the convergence process in CHP units and boilers of different hubs for an example time slot using the load-based setup. It can be seen that this setup needs 14 iterations to reach an acceptable convergence.

Fig. 12 represents the level of electrical power stored in the batteries for the load-based setup. Since the third hub (Hub #3) does not have a battery and only has heat storage, it is not shown in Fig. 12. As is shown in this figure, during the off-peak period of the day between 00:00 to 06:00 h, the batteries gradually begin to charge and during the peak hours they discharge. During the final hours of the day the storage level of the batteries reduces to the minimum allowed level. Fig. 13 represents the level of heat power stored in the heat tanks for this setup. As the second hub (Hub #2) includes only an electrical storage device, it is not shown in this figure. What is shown in this figure, similarly to Fig. 12, is that the level of stored energy in the heat tank increases and reaches its maximum level before the peak hours of the day.

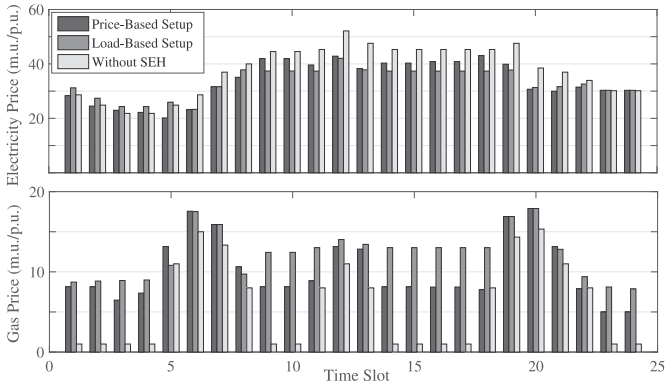

Fig. 8. Price profile of energy carriers in the two setups and without SEH.

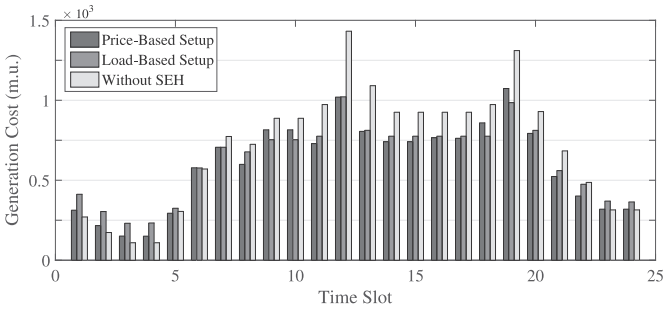

Fig. 9. Total generation cost for the two different setups and without SEH.

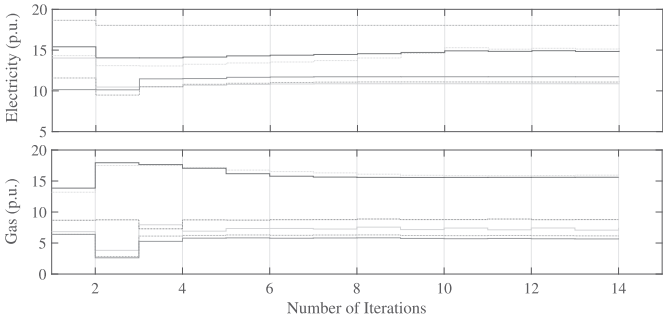

Fig. 10. Convergence of electricity and gas demand in the load-based setup for 5 energy hubs in sample time slots.

4.3. The price-based setup

Fig. 14 shows the convergence process of the price of electricity and the price of natural gas for 6 different examplary time slots by implementing the price-based setup. As can be seen, after 24 iterations the acceptable convergence is obtained.

Figs. 15 and 16 represent the level of electrical power and heat

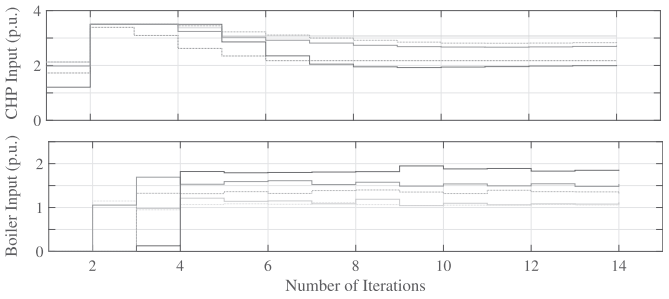

Fig. 11. Convergence of CHP and boiler inputs in the load-based setup for 5 energy hubs in sample time slots.

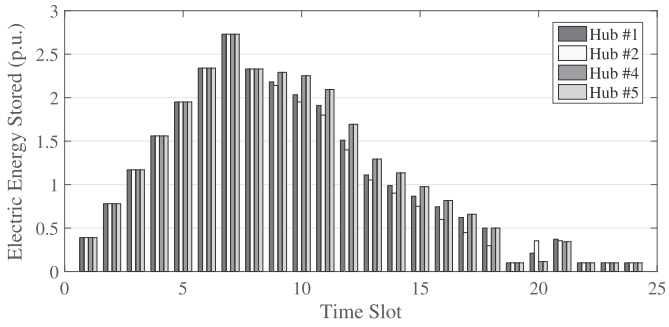

Fig. 12. Electrical energy stored in different hubs in the load-based setup.

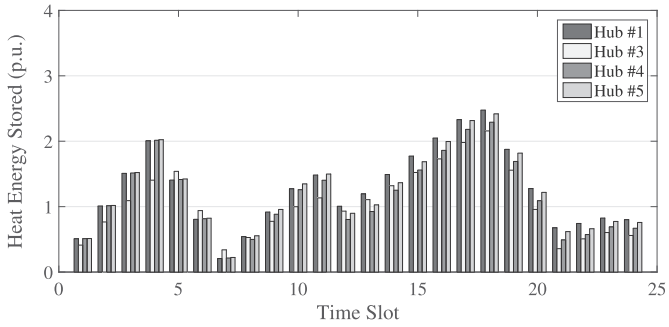

Fig. 13. Heat energy stored in different hubs in the load-based setup.

power stored in storage devices in different hubs for the proposed price-based setup. Similarly to the load-based setup, in the price-based setup both electrical and heat storage devices are charged during off-peak hours and discharged during the peak period, but with different patterns. Note that, similarly to the load-based setup, users with must-run loads can participate in this program and use storage devices for shifting their demand to the off-peak hours of a day.

4.4. Sensitivity analysis

Fig. 17 illustrates the change in total generation cost regarding up to ±20% variation of total loads. As can be seen in Fig. 17(a), by increasing the load multiplier the generation costs of the proposed setups remain lower than the situation without implementation of the SEH. Sensitivity analysis reveals that a 20% increase in the load would increase the generation cost by 2.5% and 2.2% for the load-based and price-based setups, respectively, which is lower than without implementing the SEH (a 3.5% increase). Fig. 17(b) shows

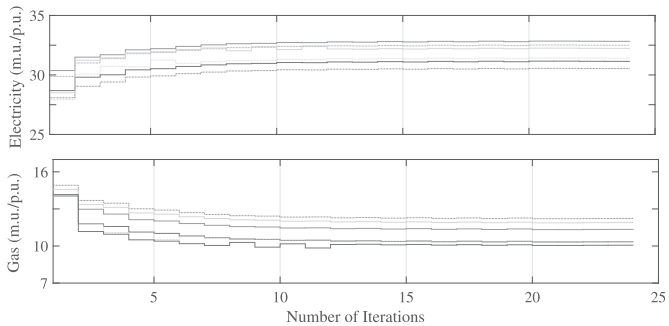

Fig. 14. Convergence of electricity and gas prices in the price-based setup for 5 energy hubs in sample time slots.

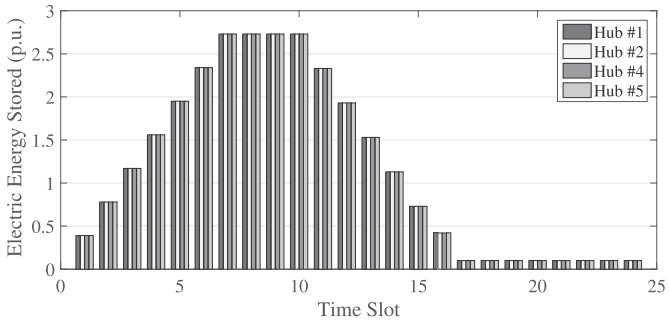

Fig. 15. Electrical energy stored in different hubs when implementing the price-based setup.

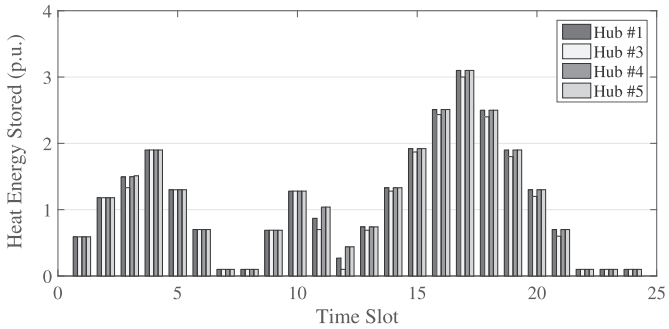

Fig. 16. Heat energy stored in different hubs when implementing the price-based setup.

the difference in the generation costs of both setups with the case where no SEH is used. As shown in this figure, these differences increase by increasing the total network load.

Fig. 18 compares the changes in total electric and natural gas demands due to the changes in electricity and natural gas prices, mimicked by changing the generation cost coefficients in Eqs. (23) and (27). In Fig. 18(a) the cost of natural gas is kept constant, and electricity costs change between −10% and 10%. As illustrated in this figure, in the load-based setup, electricity demand and gas demand are negatively and positively impacted by changes in the electricity costs. It also shows that the price-based setup is inelastic in the investigated interval. Fig. 18(b) illustrates the changes in electricity and natural gas demand induced by changes in natural gas cost. Electricity demand and gas demand is thus positively and negatively affected by changes in natural gas cost, respectively. Just like for changes in electricity costs, the price-based setup is also inelastic with regard to a change in natural gas prices in the investigated interval.

Our results indicate that electricity and gas demands vary against changes in the electricity and gas costs, showing a reverse trend. It means that by increasing the difference in the generation costs of grid-supplied electricity, the users try to minimize their energy bills by substituting natural gas for electricity.

5. Conclusion

In this paper, a novel and robust distributed algorithm has been proposed for modeling a system of interconnected smart energy hubs. The paper also describes how users can participate in integrated demand-side management. A non-cooperative congestion game model was used in which users independently optimize their energy consumption and storage schedule. To evaluate the performance of the proposed algorithm, a benchmark case with five hubs

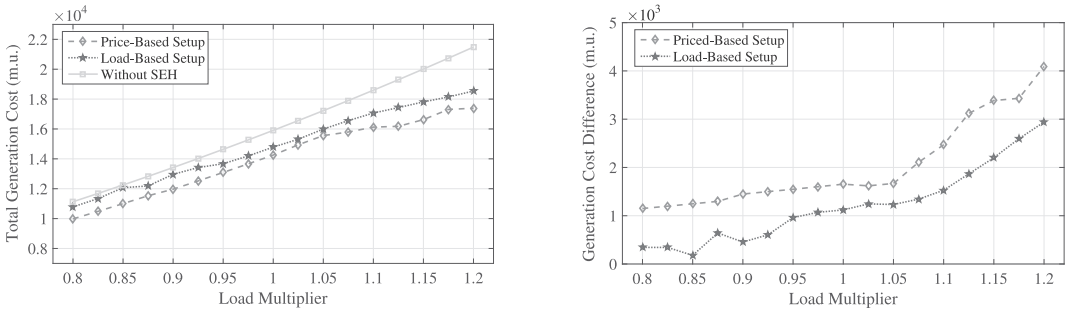

Fig. 17. Sensitivity analysis on demand; (a): Total generation cost, (b): Generation cost difference.

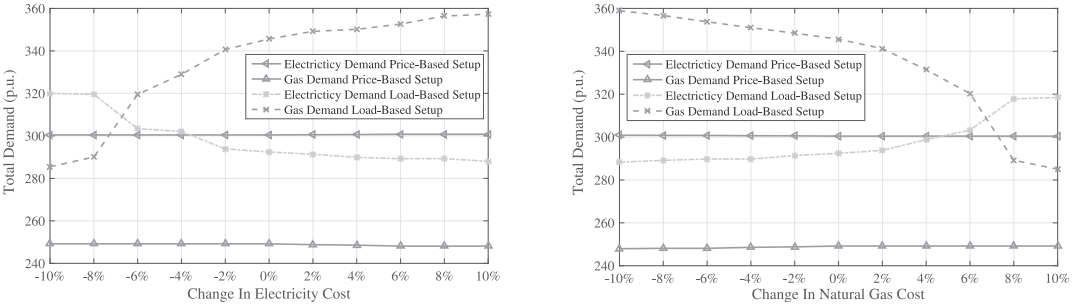

Fig. 18. Sensitivity analysis on energy cost; (a): Total demand against variations in electricity costs, (b): Total demand against variations in natural gas costs.

equipped with storage devices, including battery and heat tank, was investigated. Since this model does not converge properly due to non-convexity of the problem, an estimation function was used to decrease the gap between the maximum and minimum of the aggregated load profiles. In this model, users can take part in the program both by shifting their load demand (using storage devices) or by switching their energy sources. Moreover, connecting storage devices to an SEH was found to lead to a considerable reduction of the peak-to-average ratio for both electricity and natural gas networks.

In order to verify the effectiveness of the proposed algorithm, two different signaling schemes (i.e. price-based and load-based setup) have been introduced and compared. Both of these setups are categorized as a price-based DSM program in which the prices of energy carriers are the driving signals. Simulation results for the load-based and price-based setup, respectively, show a 27.1% and 24.4% reduction of the peak load only in the electricity networks. Furthermore, the daily energy bill is reduced by 11.9% and 15.5% in the load-based setup and price-based setup, respectively. However, the price-based setup shows more instability because of price fluctuations. Comparing the convergence rate of the two setups demonstrates that the load-based setup converges faster. The impact of variations in electricity and gas load and generation cost underline the advantages of both setups compared to a network without SEH. Moreover, since the price-based setup is inelastic to the parameter variations, it can provide lower flexibility for utility companies to control users' demand. In summary, this paper provides a useful instrument for energy utility companies to choose an appropriate configuration based on their operational constraints and policies. In future studies, the proposed algorithm can be simulated on a real system of smart energy hubs with a noticeable share of renewable energies in order to evaluate its performance. When doing so, grid parameters, such as the transmission capacity of power lines, can also be taken into account. Furthermore, the optimal signaling mechanism design for a network of interconnected energy hubs could be scrutinized.

CRediT authorship contribution statement

Seyed Omid Sobhani: Conceptualization, Methodology, Formal analysis, Investigation, Data curation, Writing - original draft, Visualization. **Siamak Sheykhha:** Conceptualization, Methodology, Formal analysis, Investigation, Data curation, Writing - original draft, Visualization. **Reinhard Madlener:** Validation, Writing - review & editing, Supervision.

Declaration of competing interests

The authors declare that they have no known competing financial interests or personal relationships that could have appeared to influence the work reported in this paper.

Acknowledgments

We are grateful for helpful comments received from reviewers and participants of the 10th International Conference on Applied Energy (ICAE 2018) held on August 22–25, 2018, in Hong Kong, China. The paper is a significantly extended version of the ICAE 2018 conference paper published in 2018 in Energy Procedia [29].

References

[1] Arnold M, Andersson G. Decomposed electricity and natural gas optimal power flow. 16th power systems computation conference (PSCC 08). Glasgow, Scotland: Citeseer; 2008.

[2] Geidl M, Koeppel G, Favre-Perrod P, Klockl B, Andersson G, Frohlich K. Energy hubs for the future. IEEE Power Energy Mag 2007;5(1):24–30.
[3] Geidl M, Koeppel G, Favre-Perrod P, Klöckl B, Andersson G, Fröhlich K. The energy hub–A powerful concept for future energy systems. Third Annual Carnegie Mellon Conference on the Electricity Industry. 2007. p. 13–4. Pittsburgh.
[4] Mancarella P. MES (multi-energy systems): an overview of concepts and evaluation models. Energy 2014;65:1–17.
[5] Sheikhi A, Bahrami S, Ranjbar AM. An autonomous demand response program for electricity and natural gas networks in smart energy hubs. Energy 2015;89:490–9.
[6] Sheikhi A, Rayati M, Bahrami S, Ranjbar A. Integrated demand side management game in smart energy hubs. IEEE Transactions on Smart Grid 2015;6(2):675–83.
[7] Bahrami S, Aminifar F. Exploiting the potential of energy hubs in power systems regulation services. IEEE Transactions on Smart Grid 2018;10(5):5600–8.
[8] Mohsenian-Rad A, Wong VWS, Jatskevich J, Schober R, Leon-Garcia A. Autonomous demand-side management based on game-theoretic energy consumption scheduling for the future smart grid. IEEE Transactions on Smart Grid 2010;1(3):320–31.
[9] Lu Q, Lü S, Leng Y. A Nash-Stackelberg game approach in regional energy market considering users' integrated demand response. Energy 2019;175:456–70.
[10] Liang Y, Wei W, Wang C. A generalized Nash equilibrium approach for autonomous energy management of residential energy hubs. IEEE Transactions on Industrial Informatics 2019;15(11):5892–905.
[11] Li R, Wei W, Mei S, Hu Q, Wu Q. Participation of an energy hub in electricity and heat distribution markets: an MPEC approach. IEEE Transactions on Smart Grid 2019;10(4):3641–53.
[12] Huang Y, Zhang W, Yang K, Hou W, Huang Y. An optimal scheduling method for multi-energy hub systems using game theory. Energies 2019;12:2270.
[13] Vahabi AR, Latify MA, Rahimiyan M, Yousefi GR. An equitable and efficient energy management approach for a cluster of interconnected price responsive demands. Appl Energy 2018;219:276–89.
[14] Wang J, Zhong H, Ma Z, Xia Q, Kang C. Review and prospect of integrated demand response in the multi-energy system. Appl Energy 2017;202:772–82.
[15] Mukherjee U, Walker S, Maroufmashat A, Fowler M, Elkamel A. Power-to-gas to meet transportation demand while providing ancillary services to the electrical grid. Smart Energy Grid Engineering (SEGE). IEEE; 2016. p. 221–5.
[16] Zhang X, Karady GG, Ariaratnam ST. Optimal allocation of chp-based distributed generation on urban energy distribution networks. IEEE Transactions on Sustainable Energy 2014;5(1):246–53.
[17] Tingji C, Anping T, Yuhuai W, Guojie L, Jing X. A multiport energy hub for the connection of multi power flow: a simulating case. In: IEEE Conference on Energy Internet and Energy System Sntegration (EI2), 2017. IEEE; 2017. p. 1–5.
[18] Aghamohamadi M, Mahmoudi A. From bidding strategy in smart grid toward integrated bidding strategy in smart multi-energy systems, an adaptive robust solution approach. Energy 2019;183:75–91.
[19] Bahrami S, Toulabi M, Ranjbar S, Moeini-Aghtaie M, Ranjbar AM. A decentralized energy management framework for energy hubs in dynamic pricing markets. IEEE Transactions on Smart Grid 2018;9(6):6780–92.
[20] Noor S, Yang W, Guo M, van Dam KH, Wang X. Energy demand side management within micro-grid networks enhanced by blockchain. Appl Energy 2018;228:1385–98.
[21] Pipattanasomporn M, Kuzlu M, Rahman S, Teklu Y. Load profiles of selected major household appliances and their demand response opportunities. IEEE Transactions on Smart Grid 2013;5(2):742–50.
[22] Motalleb M, Ghorbani R. Non-cooperative game-theoretic model of demand response aggregator competition for selling stored energy in storage devices. Appl Energy 2017;202:581–96.
[23] Wang F, Xiang B, Li K, Ge X, Lu H, Lai J, Dehghanian P. Smart households' aggregated capacity forecasting for load aggregators under incentive-based demand response programs. IEEE Trans Ind Appl 2020;56(2):1086–97.
[24] Zhen Z, Pang S, Wang F, Li K, Li Z, Ren H, et al. Pattern classification and PSO optimal weights based sky images cloud motion speed calculation method for solar PV power forecasting. IEEE Trans Ind Appl 2019;55(4):3331–42.
[25] Li K, Wang F, Mi Z, Fotuhi-Firuzabad M, Duić N, Wang T. Capacity and output power estimation approach of individual behind-the-meter distributed photovoltaic system for demand response baseline estimation. Appl Energy 2019;253:113595.
[26] San-Salvador Á, Herrero Á. Contacting the devices: a review of communication protocols. In: Novais P, Hallenborg K, Tapia DI, Rodríguez JMC, editors. Ambient intelligence - software and applications. Berlin, Heidelberg: Springer Berlin Heidelberg; 2012.
[27] Wu C, Mohsenian-Rad H, Huang J, Wang AY. In: Demand side management for wind power integration in microgrid using dynamic potential game theory. IEEE GLOBECOM Workshops (GC Wkshps); 2011. p. 1199–204. 2011.
[28] Wood AJ, Wollenberg BF. Power generation, operation, and control. John Wiley & Sons; 2013.
[29] Sobhani SO, Sheykhha S, Azimi MR, Madlener R. Two-level distributed demand-side management using the smart energy hub concept. Energy Procedia 2019;158:3052–63.
[30] Rosenthal RW. A class of games possessing pure-strategy Nash equilibria. Int J Game Theory 1973;2:65–7.